



Akademie věd
České republiky

Teze disertace
k získání vědeckého titulu “doktor věd”
ve skupině věd: *fyzikálně-matematických*

Geometry induced phase transitions at patterned surfaces

Komise pro obhajoby DSc. disertací v oboru *Fyzika kondenzovaných systémů*

Jméno uchazeče: *doc. Mgr. Alexandr Malijeuský, Ph.D.*

Pracoviště uchazeče: *Vysoká škola chemicko-technologická v Praze*

Praha, 2018

Contents

1	Summary	1
2	Introduction	2
3	Bulk Critical Phenomena	4
4	Interfacial Phase Transitions: A Planar Geometry	7
4.1	Wetting phenomena	7
4.2	Capillary condensation	15
5	Classical Density Functional Theory	18
6	Interfacial Phase Transitions: A Non-Planar Geometry	21
6.1	Linear wedges and edges	22
6.2	Capillary grooves	30
6.3	Rough surfaces	35
6.4	Bridging transitions	36
7	Conclusions	38
8	List of selected publications	39

1 Summary

The objective of the doctoral thesis is to present my contribution to the theory of interfacial phase transitions. In this thesis, I will put my research into a broader context, including a historical development of the field. To this end, the thesis starts with a brief summary of the main properties of bulk phase transitions, i.e. those occurring in macroscopically large and uniform systems. Eventually, I will turn to a description of the phenomenology of surface phase transitions in a planar geometry. These include wetting transitions and capillary condensation; in both cases, an ambient (or bulk) fluid is considered to be a low-density (gas) phase but a geometry restriction due to the presence of the confining wall(s) and the corresponding wall-fluid interaction induce a formation of a high-density liquid-like phase that would be metastable in bulk. In order to link these and related phenomena with the microscopic properties of the matter, an appropriate statistical-mechanical tool is needed, which I briefly introduce. The main part of the thesis is devoted to a description of interfacial phenomena at non-planar model walls. This primarily includes wedge and groove filling transitions, wetting at periodically patterned walls and bridging transitions between two spherical or cylindrical walls. The nature of these transitions, criticality and the effect of thermal fluctuations are discussed and a brief summary including perspective of the field is provided in the final part of the thesis.

2 Introduction

The presented dissertation belongs to the field of statistical physics of liquids applied to phenomena, and phase transitions in particular, that occur on surfaces where two bulk phases meet. In most cases, we will deal with a solid-gas interface, at which, under certain circumstances, a liquid phase nucleates. A theoretical basis of these *wetting phenomena* has been formed already in nineteenth century and is associated with the classical works of T. Young and P.-S. Laplace. Within their fully macroscopic treatment, the wetting behaviour of solid walls, i.e. their affinity to adsorb liquid, is provided by phenomenological quantities such as contact angle, surface tension etc. In particular, it was shown that the contact angle θ of a sessile drop sitting on a planar solid wall is given by balancing surface tensions at the wall-liquid-gas coexisting line. However, it was not before the 70's of the last century, when it turned out that a change from a *partial wetting* state ($\theta > 0$) into a *complete wetting* state ($\theta = 0$) at bulk two-phase coexistence pressure (or, equivalently, chemical potential) is an example of a *surface phase transition*. From a statistical mechanical viewpoint this means that the (surface) free energy of such a system (which can be linked directly with the contact angle θ) exhibits singularity at this thermodynamic point. Interestingly, the very beginning of this new field of wetting transitions was accompanied by a controversy about the order of the transition. While the Cahn model predicted that the transition is first-order [1, 2], such that the slope of the contact angle changes abruptly and the latent heat is released, a more microscopic Sullivan's model [3, 4, 5] showed that the transition is continuous (the singular behaviour of the free energy is then shifted to higher derivatives). Using scaling methods [6] and a fully microscopic classical density functional theory (DFT) [7] the debate was resolved in early 80's with a compromise: the order of the transition depends on the character of the microscopic (intermolecular) forces and both scenarios are possible, although the first-order wetting transitions are much more abundant in nature.

After three decades of an intense theoretical scrutiny it may be concluded that wetting phenomena at planar solid walls are sufficiently well understood [8]; this includes a description of possible phase transitions and corresponding fluctuating regimes, their nature and a connection with microscopic properties of the matter. More recently, however, fluid condensation at structured or nano-patterned surfaces attracted a considerable interest. There are at least

two reasons for that. Firstly, the wall geometry can have a dramatic impact on the fluid phase behaviour; it reveals that even a microscopic corrugation and roughness of the wall may change location and order of the phase transitions or even induce completely new phenomena that are absent in the planar case. Clearly, on a microscopic scale any solid surface is rough and thus our knowledge of surface phenomena on perfectly smooth walls should be thought only as a first approximation towards understanding of fluid adsorption on real surfaces. Secondly, with advanced techniques in nanolithography [9, 10] that enable modification of the shape of solid surfaces even on a molecular scale, the understanding of fluid phase behaviour near such modified surfaces becomes important in view of modern technologies such as micro- and nanofluidics [11].

A description of fluid phase behaviour near structured surfaces turned to be an extremely complex and non-trivial task. One obvious reason for this is that a non-planar geometry breaks symmetry of the system along at least one dimension which makes the analysis much more complicated compared to the planar case. Another specific aspect of these systems is that the underlying phase behaviour is very sensitive to the geometric details of the wall. For example, adsorption at sinusoidally shaped walls was shown to exhibit so called unbending transition [12]; in this case, the shape of the liquid-gas interface, which forms above the liquid film intruding between the wall and the ambient gas, follows initially the shape of the wall and grows continuously as the pressure is increased. However, at some point the interface changes its shape abruptly and flattens; this is an example of a geometry-induced (first-order) phase transition. If, in contrast, the shape of the wall is “saw-tooth”, there is no such an unbending transition and the sinusoidal undulation of the liquid-gas interface persists, although its amplitude decreases continuously with the film height.

A general task for a theorist is to address several questions. First of all, we wish to know what kind of (surface) phase transitions such a given model wall may induce and under which conditions. Furthermore, we want to know what is the nature of the transitions and if continuous, to quantify the divergence of the pertinent quantities by determining the associated critical exponents. The values of the critical exponents can be both universal or may depend on the character of the microscopic interactions; in the latter case, obviously, a microscopic approach needs to be applied. It is also important to show if/that there exists “hidden symmetries” between various apparently very distinct interfacial transitions, but which we can describe in a formally same way with

identical values of critical exponents.

In the remainder of the thesis I will start with a brief overview of the bulk critical phenomena (section 2) which is followed by a concise introduction to the theory of wetting transitions and capillary condensation (section 3), i.e. two fundamental examples of surface phase transitions in a planar geometry. In section 4 I will mention some of the main theoretical methods which I have used in works that are discussed in section 5. These are the interfacial phenomena in non-planar confining geometries and the corresponding list of publications concludes the thesis.

3 Bulk Critical Phenomena

Bulk phase transitions and critical phenomena occur in macroscopic systems where the matter is not affected by the presence of external fields and boundaries, and thus the distribution of the matter is uniform on average. In figure 1 a typical sketch of the phase diagram in the pressure-temperature projection is shown; the lines represent phase boundaries where two distinct phases can coexist. By crossing the phase boundaries, the system undergoes first-order phase transition during which its macroscopic properties change abruptly. The liquid-vapour line terminates at the *critical point* beyond which no distinction between the two phases can be made. This means that the coexistence line can be bypassed in a path connecting two distinct fluid phases. This contrasts with the solid-liquid and solid-vapour transitions since in these cases the two phases possess different symmetry. The phenomena that occur near the critical point are called critical phenomena and are characterised by strong fluctuation effects and by a power-law divergence of certain quantities which can be quantified by *critical exponents*. Generally, two phases that occur near the critical point are distinguished by the *order parameter* which is typically zero in one (less ordered) phase and non-zero in another phase. In particular, for the liquid-vapour system the order parameter is the density difference between the two phases, $\rho_L - \rho_V$, so that its value is zero above the critical temperature T_c and non-zero below. By defining the reduced temperature $t = (T_c - T)/T_c$, the critical behaviour near the liquid-vapour critical point is characterized by the following relations and critical exponents:

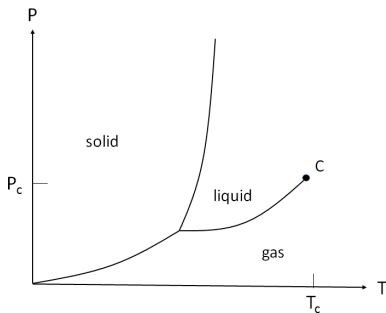


Figure 1: Temperature-pressure phase diagram of a simple substance. All the transitions are discontinuous except at the critical point (C).

- Specific heat: $C_v \propto |t|^{-\alpha}$ as $t \rightarrow 0$ at $\rho = \rho_c$;
- Density difference: $\rho_L - \rho_V \propto t^\beta$ as $t \rightarrow 0$;
- Isothermal compressibility: $\chi_T \propto |t|^{-\gamma}$ as $t \rightarrow 0$;
- Critical isotherm: $\rho_L - \rho_V \propto |P - P_c|^{1/\delta}$ as $P \rightarrow P_c$ at $t = 0$;
- Correlation length: $\xi \propto |t|^{-\nu}$ as $t \rightarrow 0$;
- Density-density correlation function: $G(r) \propto \frac{1}{r^{d-2+\eta}}$ at $t = 0$.

The concept of the critical point was introduced in 1869 when Andrews presented his experimental results on carbon dioxide [13]. Soon after, van der Waals formulated first microscopic theory for fluid phase behaviour in which the critical point was included [14]. Almost simultaneously, the critical point¹ emerged also in the theory of ferromagnets proposed by Weiss. These advances revealed a very interesting similarity between fluids and magnets; when the pressure is taken as the analogue of magnetic field H and the pressure difference as the analogue of magnetization M , the two theories exhibit notably similar critical behaviour. Even more remarkably, van der Waals and Weiss theories turned out to provide an identical set of critical exponents. The close

¹For magnets, the critical point or critical temperature is often termed as Currie point and Currie temperature, respectively.

analogy between the two theories, describing entirely disparate systems, was eventually explained by the Landau theory [15] of continuous phase transitions. The Landau theory, based solely on a few simple phenomenological assumptions, proved to be extraordinary useful. In fact, the Landau theory became a synonym to all mean-field (MF) theories, which do not account properly (or neglect at all) for long-range fluctuations, since any MF theory is only a specific case of the general Landau theory. However, the effect of fluctuations near the critical point is generally important, hence the MF theories are not exact and the so called classical critical exponents which they predict do not match with real experiments.

The behaviour of equilibrium systems with many degrees of freedom is most conveniently described by means of statistical mechanics. Formally, the general strategy of the statistical-mechanical treatment is very straightforward: all, what is needed, is to evaluate the *partition function*

$$Z = \text{Tr} e^{-\beta\mathcal{H}}, \quad (1)$$

where \mathcal{H} is the Hamiltonian governing the system and $\beta = 1/k_B T$ is the inverse temperature with k_B being the Boltzmann constant. Taking derivatives of Z , all thermodynamic properties of the system and its fluctuation behaviour can be determined. However, when it comes to *continuous phase transitions*, it reveals that their behaviour are largely insensitive to the details of the model and their nature, characterised by the critical exponents, are same even for a large number of diverse systems that constitute a given *universality class*. Hence, even very simple, “minimal” models, such as the famous Ising model, can be used to describe critical behaviour of many systems. The Ising model is defined by the Hamiltonian [16]

$$\mathcal{H} = -J \sum_{\langle ij \rangle} S_i S_j - H \sum_i S_i, \quad (2)$$

where J is the interaction parameter and where the degrees of freedom $S_i = \pm 1$ are assumed to interact only with their nearest-neighbours. An exact solution of the Ising model in two dimensions by L. Onsager (1944) [17] showed that the mean-field (Landau-type) theories provide only approximative values of the critical exponents and cannot be considered as fully satisfactory.

The fail of the “classical era” of the theory of critical phenomena induced a great challenge for a formulation of an alternative theory which would properly

incorporate an impact of thermal fluctuations. This effort proved to be highly non-trivial, as it occurred that no extension of the previous methods is satisfactory but rather a completely new approach is needed. Such a theory should e.g. explain, why the critical exponents are not independent but are linked by certain identities. As first shown by Widom (1965) [18], the existence of the exponent relations can be explained by assuming *scaling* properties of the free energy near the critical point. This Widom's hypothesis also explains why binodals of different systems collapse to a single curve near the critical temperature when expressed in appropriately re-scaled units. The origin of the scaling has been heuristically explained by Kadanoff (1966) [19] who introduced the block-spin idea that have been further elaborated by Wilson (1971) who formulated the famous *renormalization-group* (RG) theory [20, 21, 22]. The RG theory proved to be a method by which one can estimate the values of the critical exponents in a systematic way. Moreover, it explains the origin of scaling and universality, and reveals the importance of the system dimensionality d , the critical exponents are generally dependent on. In particular, every critical system possesses the *upper critical dimension*, d^* , such that the effect of fluctuations is not essential for $d > d^*$ where the mean-field theories thus become exact.

4 Interfacial Phase Transitions: A Planar Geometry

4.1 Wetting phenomena

Consider a planar wall² onto which some amount of liquid is poured. From a macroscopic viewpoint the wetting properties of the wall can be characterised by the contact angle θ at which the liquid drop meets the wall. If $\theta > 0$, the system is in a *partial wetting* regime and the liquid forms a hemispherical cap³. Balancing the net force per unit length acting along the boundary line between the three phases, the equilibrium contact angle is given by Young's

²The wall is typically assumed to be of a solid material although this assumption is not necessary at this point.

³If not stated otherwise, we will implicitly consider only hydrophilic walls, such that $\theta < \pi/2$. In the opposite case, the wall is called to be dried (i.e., wetted by the vapour) which is just a reverse phenomenon to wetting.

equation

$$\gamma_{wg} = \gamma_{wl} + \gamma \cos \theta, \quad (3)$$

in terms of the tensions of the wall-vapor, wall-liquid and liquid-vapour interfaces. If adsorption properties of the wall are strong enough, the system can exhibit *wetting transition* at a wetting temperature T_w at which the wall surface becomes completely wet and $\theta = 0$. Eq. (3) then becomes Antonow's equation:

$$\gamma_{wg} = \gamma_{wl} + \gamma, \quad (4)$$

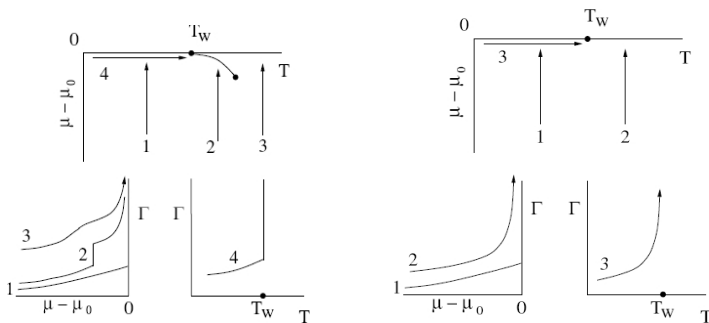


Figure 2: Phase diagrams of a first order (left) and a continuous (right) wetting transition. Also shown are representative thermodynamic paths on diagrams below. The difference $\mu - \mu_0$ measures the departure in the chemical potential from bulk two-phase coexistence and the adsorption Γ is proportional to the liquid film thickness ℓ_π .

Alternatively, the wetting transition can be viewed as an intrusion of a liquid layer into a wall-vapour interface [23, 24, 25]. The partial wetting regime corresponds to a finite value of the liquid film thickness ℓ_π or, equivalently, the surface adsorption Γ . The film thickness (or adsorption) serves as the natural order parameter for the wetting transition, at which ℓ_π (or Γ) diverges (in the absence of gravity). There are two possible ways how the divergence can be realized:

- The wetting temperature is approached from below, $T \rightarrow T_w^-$, along the bulk liquid-vapour coexistence line, such that the chemical potential $\mu = \mu_0(T)$, where $\mu_0(T)$ is the saturation chemical potential at a given temperature. This transition can be either discontinuous, i.e. *first-order wetting* (figure 2, left panel, path No. 4) or continuous – usually called *critical wetting* (figure 2, right panel, path No. 3). Clearly, the free energy is non-analytic at T_w in both cases and its singular part which is defined as

$$f_{\text{sing}} = \gamma_{\text{wg}} - (\gamma_{\text{wl}} + \gamma) \quad (5)$$

vanishes at T_w according to

$$f_{\text{sing}} \sim t^{2-\alpha_s}, t > 0, \quad (6)$$

where $t \equiv (T_w - T)/T_w$. For further purposes, it is useful to note that by combining (3) and (5) we obtain

$$f_{\text{sing}} \approx -\frac{\gamma\theta^2}{2} \quad (7)$$

near T_w where the contact angle is small.

The value of the critical exponent α determines the order of the transition. From Eqs. (3) and (6) it follows that

$$1 - \cos \theta \sim t^{2-\alpha_s}, t > 0. \quad (8)$$

Now, the derivative of the contact angle with respect to the temperature,

$$\frac{d \cos \theta}{dT} \sim t^{1-\alpha_s}, \quad (9)$$

must be continuous at T_w for critical wetting (no latent heat) and therefore $\alpha_s < 1$. For first-order wetting, there is a latent heat at the transition, $\cos \theta$ is therefore discontinuous at T_w and $\alpha_s = 1$. For critical wetting we also define the critical exponent β_s which characterises the divergence of the film thickness (or adsorption) as T approaches T_w :

$$\ell_\pi \sim t^{-\beta_s}. \quad (10)$$

- The bulk liquid-vapour coexistence is approached from below at a fixed temperature $T_w < T < T_c$ (the lines Nos. 2 and 3 in the left panel and the line No. 2 in the right panel of figure 2). Within this process, the thickness of the liquid layer diverge as $\mu \rightarrow \mu_0^-$ according to the power-law

$$\ell_\pi(\delta\mu) = \delta\mu^{-\beta_s^{\text{co}}}, \quad (11)$$

where $\delta\mu = \mu_0 - \mu$. This continuous divergence of the liquid film is called *complete wetting*. For the singular part of the free energy, we have by analogy with Eq. (6):

$$f_{\text{sing}} \sim \delta\mu^{2-\alpha_s^{\text{co}}}, \delta\mu > 0. \quad (12)$$

For the first-order wetting transitions, the singularity in the surface free energy at T_w extends above T_w and below μ_0 to a pre-wetting line which is the locus of coexistence between two distinct phases with thin and thicker wetting layers. This line terminates at its own critical temperature T_{sc} and approaches the coexistence line tangentially at T_w as $\delta\mu \sim (T - T_w)^{\frac{3}{2}}$.

In general, the surface critical exponents depend on the range of the fluid-fluid and wall-fluid interactions. Our main focus will be on models where the interaction between molecules is long-ranged (decaying as a power-law at infinity), with a particular emphasis on the most relevant case where the particles interact via van der Waals (dispersion) forces.

Wetting phenomena (in d dimensions) can be studied using the interfacial Hamiltonian model in terms of the height $\ell(x)$ of the liquid-gas interface (i.e., the local wetting film thickness)

$$\mathcal{H}_\pi[\ell] = \int d\mathbf{x} \left[\frac{\gamma}{2} (\nabla\ell)^2 + W(\ell) \right], \quad (13)$$

where \mathbf{x} denotes the $(d-1)$ coordinates parallel to the wall. The first term in the integral is the energy cost of an undulation of the interface due to thermal fluctuations that are assumed to be small ($|\nabla\ell| \ll 1$). The second term, $W(\ell)$, represents effective interaction of the interface with the wall and is called *binding potential*. For the long range interactions, the binding potential has the asymptotic form:

$$W(\ell) = \frac{a(T)}{\ell^p} + \frac{b(T)}{\ell^q} + \dots; \ell > 0, \quad (14)$$

where $p = 2$ and $q = 3$ for (non-retarded) van der Waals forces in three dimensions⁴. This binding potential is appropriate as far as two-phase coexistence is concerned, i.e, for $\mu = \mu_0$; this is the case of first-order or critical wetting. For complete wetting, we have $\mu < \mu_0$, and the energy cost for the presence of the metastable liquid must also be included:

$$W(\ell) = \delta\mu(\rho_l - \rho_g)\ell + \frac{a(T)}{\ell^p} + \dots; \ell > 0. \quad (15)$$

If the interfacial fluctuations are neglected, $\ell(\mathbf{x}) = \text{const}$, and the equilibrium wetting configuration is given simply by minimising the binding potential. The system is wet if the minimum corresponds to ℓ infinite which requires $a(T) > 0$. There are two mechanisms by which this global minimum can shift to a finite value of ℓ . The first mechanism can occur as $a(T)$ changes its sign with $b(T)$ positive. If $a(T) < 0$, the binding potential approaches zero asymptotically from below, which means that the minimum is at finite value of $\ell \sim a^{-1}$; the wall is not wet. However, as $a(T) \rightarrow 0$, the film thickness grows continuously and eventually diverges at T_w for which $a(T_w) = 0$ and $b(T_w) > 0$. Clearly, this mechanism corresponds to critical wetting. Note that as $a(T)$ changes its sign at the wetting temperature, $a \sim t$. From this it follows that $\beta_s = 1$ and upon substituting into (14) and (12) we get $\alpha_s = -1$ for van der Waals forces.⁵ The second mechanism is realized if $b(T) < 0$ (or if the coefficient of a higher-order term in the expansion (14) is negative) and $a(T) > 0$, in which case the binding potential exhibits two minima at ℓ finite and ℓ infinite. In this case, T_w corresponds to the temperature below which finite ℓ minimum becomes the global minimum. This is the case of a first-order wetting. This mechanism is pertinent for systems in which the only forces that are long range are those between fluid and wall atoms; in this case $a(T)$ remains always positive. For complete wetting, the term linear in ℓ prevents from unbinding of the interface for any positive value of $\delta\mu = \mu_0 - \mu$. The wall thus becomes completely wet only in the $\mu \rightarrow \mu_0$ limit with the associated critical exponents $\alpha_s^{\text{co}} = 4/3$ and $\beta_s^{\text{co}} = 1/3$ for van der Waals forces.⁶ Note that all terms beyond the ℓ^{-p} order are irrelevant for complete wetting.

The MF analysis can be complemented by the OZ approximation to obtain further critical exponents related with the structure of the interface. The OZ

⁴The coefficient $a(T)$ is often termed the Hamaker constant.

⁵More generally: $\alpha_s = (2 - 2p)/(q - p)$ and $\beta_s = 1/(q - p)$.

⁶More generally: $\alpha_s^{\text{co}} = (p + 2)/(p + 1)$ and $\beta_s^{\text{co}} = 1/(p + 1)$.

theory corresponds to the functional Taylor expansion of $\mathcal{H}_\pi[\ell]$ up to second order in fluctuations $\delta\ell(\mathbf{x}) = \ell(\mathbf{x}) - \ell_\pi$ around the mean value of the interface height $\langle\ell\rangle = \ell_\pi$. From this it follows that the transverse correlation length, defined by the OZ theory as

$$\gamma\xi_{\parallel}^{\xi^{-2}} \equiv \left. \frac{d^2W(\ell)}{d\ell^2} \right|_{\ell=\ell_\pi} \quad (16)$$

behaves as

$$\xi_{\parallel} \sim t^{-\nu_{\parallel}}, \quad (\text{critical wetting}) \quad (17)$$

with $\nu_{\parallel} = 5/2$ for critical wetting and

$$\xi_{\parallel} \sim \delta\mu^{-\nu_{\parallel}^{\text{co}}}, \quad (\text{complete wetting}) \quad (18)$$

with $\nu_{\parallel}^{\text{co}} = 2/3$ for complete wetting.⁷

The MF theory is no longer correct when the fluctuation effects become important. The upper critical dimension where the MF theory ceases to hold, can be determined using the Ginzburg criterion. The contribution of the fluctuations to the surface free energy can be estimated as

$$f_s^f \approx k_B T / \xi_{\parallel}^{d-1} \sim t^{(d-1)\nu_{\parallel}}. \quad (19)$$

If compared with (6), we obtain the hyper-scaling relation

$$2 - \alpha_s = (d-1)\nu_{\parallel} \quad (20)$$

and, similarly, for complete wetting:

$$2 - \alpha_s^{\text{co}} = (d-1)\nu_{\parallel}^{\text{co}}. \quad (21)$$

The hyper-scaling relations are only valid for the MF critical exponents for $d = d^*$ and therefore

$$d^* = \frac{3q+2}{q+2} \quad (\text{critical wetting}) \quad (22)$$

and

$$d^* = \frac{3p+2}{p+2} \quad (\text{complete wetting}). \quad (23)$$

⁷More generally: $\nu_{\parallel} = (q+2)/(2(q-p))$ and $\nu_{\parallel}^{\text{co}} = (p+2)/(2p+2)$.

For van der Waals forces, $d^* = 11/5$ for critical wetting and $d^* = 2$ for complete wetting. These results are important because they tell us that the MF theory of wetting is exact in $d = 3$ for long-range forces.

Although the MF theory of wetting is exact in the most relevant case of a three-dimensional system with long-range forces,⁸ it is nevertheless desirable to account for the effect of fluctuations in systems of lower space dimensions. As we will see later on, this may occur to be very useful for a description of other interfacial phenomena that can be effectively mapped onto wetting phenomena at reduced dimensions. To properly include the fluctuations, exact transfer-matrix or approximate RG techniques have often been employed but much about their influence can be learnt from the simple arguments that I will demonstrate for dimension $d = 2$.

Fluctuations in ℓ decays in a distance of ξ_{\parallel} and thus for the first term in Eq. (13) we have

$$\frac{\gamma}{2}(\nabla\ell)^2 \sim \frac{\ell^2}{\xi_{\parallel}^2}. \quad (24)$$

The fluctuations become important when $\ell \sim \xi_{\perp}$ where

$$\xi_{\perp} = \sqrt{\langle \ell(x)^2 \rangle - \ell_{\pi}^2} \quad (25)$$

is the perpendicular correlation length or roughness. The transverse and correlation lengths are related through the wandering exponent as $\xi_{\perp} = \xi^{\zeta}$, so that

$$\frac{\gamma}{2}(\nabla\ell)^2 \sim \frac{\ell^2}{\xi_{\parallel}^2} \sim \ell^{-\tau}, \quad (26)$$

with $\tau = 2/\zeta - 2$. Adding this interaction term due to fluctuations to the binding potential with long-range forces (14), we obtain an effective potential:

$$W_{\text{eff}}(\ell) = \frac{a(T)}{\ell^p} + \frac{b(T)}{\ell^q} + \frac{c(T)}{\ell^{\tau}}; \ell > 0. \quad (27)$$

Thus beside the two first energy terms that describe a direct interaction between the interface and the wall, we also have a competing term which includes an entropy loss due to the wall presence accounting for the restricted number

⁸For systems with short-range forces $d^* = 3$ for both critical and complete wetting. In this case, the critical singularities are $\alpha_s = 0$, $\beta_s = 0(\ln)$ and $\nu_{\parallel} = 1$ and $f_s^{\text{co}} = \delta\mu \ln \delta\mu$, $\beta_s^{\text{co}} = 0(\ln)$ and $\nu_{\parallel}^{\text{co}} = 1/2$.

of possible fluctuations of a bound state compared to an unbound state. The last term in (27)) is therefore repulsive, hence $c(T) > 0$ and it can be shown that $\tau = 2$ for $d = 2$. Depending on the values of p and q relative to τ , we obtain three scaling regimes for critical wetting [26]:

1. $\tau > q$: *Mean-field regime*. Since the critical exponents for critical wetting are given by the first two terms in the binding potential, the fluctuation term has no effect and the MF theory is exact in this regime.
2. $p < \tau < q$: *Weak-fluctuation regime*. Now the fluctuation term is second largest and the critical exponents (that are now dimension-dependent) are not correctly predicted by the MF theory. However, the critical temperature which is given by the leading order term, is still given correctly by the MF theory and the critical exponents can be obtained from the MF theory by replacing $q \rightarrow \tau$; in particular, $\beta_s = 1/(\tau - p)$.
3. $\tau < p < q$: *Strong-fluctuation regime*. In this regime, the fluctuation term is dominating and even the location of the wetting temperature is not correctly given by MF theory. For $d = 2$ when ℓ is a function of a single coordinate, the transfer-matrix method can be employed which transforms the statistical mechanical problem to the eigenvalue problem for the Schrödinger equation:

$$\left(\frac{1}{\gamma\beta^2} \frac{d}{d\ell^2} + W(\ell) \right) \psi_n(\ell) = E_n \psi_n(\ell), \quad (28)$$

to determine $P(z) = |\psi_0(z)|^2$, the probability to find the interface at a height z .

For complete wetting, the situation is simpler, since only the leading order term in the binding potential is important for the critical exponents. This can be viewed from the fact that the binding potential (15) can be formally obtained from (14) by taking $a = \delta\mu$ and $p = -1$. As the leading order term is thus always lower than τ , there is no strong-fluctuation regime for complete wetting. For a fixed dimension $d < 3$, there is a marginal value $p^* = 2(d - 2)/(3 - d)$ of the exponent p , such that:

1. $p < p^*$: *Mean-field regime*. The MF theory is valid and the critical behaviour is determined by minimization of $W(\ell)$.

2. $p > p^*$: *Weak-fluctuation regime*. For systems with shorter-range forces than those corresponding to p^* fluctuation effects dominate. According to the RG theory, $\beta_s^{\text{co}} = (3 - d)/(d + 2)$.

4.2 Capillary condensation

Consider a pair of parallel infinite planes that are a distance L apart and which is embedded inside the bulk gas reservoir chemical potential μ (pressure p). We assume that the temperature of the system is $T < T_c$, so that the *bulk* system experiences first-order liquid-vapour phase transition at the chemical potential $\mu_0(T)$. In contrast, the confined gas exhibits first-order condensation transition at a *shifted* value of $\mu_{cc}(T; L)$ which is macroscopically given by the classical Kelvin equation

$$\mu_{cc}(T; L) = \mu_0(T) - \frac{2(\gamma_{wg} - \gamma_{wl})}{L\Delta\rho} \quad (29)$$

where $\Delta\rho = \rho_l - \rho_g$ is the difference between the particle densities of the bulk liquid and gas coexisting phases. We will further assume that $\gamma_{wg} > \gamma_{wl}$, i.e. that the walls favour liquid and thus on using of (3)

$$\mu_{cc}(T; L) = \mu_0(T) - \frac{2\gamma \cos\theta}{L\Delta\rho} \quad (30)$$

with $\cos\theta > 0$, implying $\mu_{cc} < \mu_0$. Such a proces, within which a low-density gas-like state changes abruptly into a dense liquid-like state, is called *capillary condensation*. The opposite case, *capillary evaporation*, occurs when the walls favour gas and then the opposite inequalities apply.

There are two ways how the Kelvin equation can be derived. Within the thermodynamic treatment, and for large L , we can write for the grand potential per unit area of the low-density state at the pressure p and chemical potential μ

$$\omega_g \approx -pL + \gamma_{wg} \quad (31)$$

and for the liquid-like state

$$\omega_l \approx -p^\dagger L + \gamma_{wl} \quad (32)$$

where p^\dagger is the pressure of the metastable bulk liquid at the same chemical potential μ . By balancing ω_g and ω_l and using 3, a first-order condensation

occurs at the pressure p satisfying

$$p - p^\dagger = \frac{2\gamma \cos \theta}{L}. \quad (33)$$

Finally, assuming that the undersaturation $\delta\mu = \mu_0 - \mu_{cc}$ at which the transition occurs is small, we can expand both p and p^\dagger around the saturation pressure to first order leading to $p - p^\dagger \approx \delta\mu\Delta\rho$, which upon substituting to (33) reproduces (30).

Alternatively, the macroscopic Kelvin equation can be derived using geometric arguments. Right at the capillary condensation μ_{cc} the two low-density and high-density states may coexist. The presence of the liquid-like state, which is metastable in bulk, necessitates the presence of a meniscus at the “liquid-gas” interface. In the macroscopic limit $L \rightarrow \infty$, the meniscus must satisfy two conditions: i) it meets the walls at Young’s contact angle θ and ii) its radius of curvature is the Laplace radius $R = \gamma/(p - p^\dagger) \approx \gamma/(\delta\mu\Delta\rho)$. Since for the slit pore $L = 2R$, we obtain (30) again.

As we could see, both derivations assume the macroscopic limit $L \rightarrow \infty$ and it is only in this limit when the Kelvin equation (30) is reliable. A more microscopic approach which takes into account also a singular part of the interfacial tensions, leads to a more accurate prediction, when the walls are completely wet ($\theta = 0$). In this case, the wetting layers form at the walls, the width of which grow as $\ell_\pi \sim (\mu_0 - \mu)^{-1/3}$ in the limit of $L \rightarrow \infty$ for walls exerting van der Waals forces. The presence of such films in the slit leads to a modified Kelvin equation valid for large L :

$$\mu_{cc}(T; L) = \mu_0(T) - \frac{2\gamma}{(L - 3\ell_\pi)\Delta\rho} \quad (34)$$

That L should be replaced by $L - 3\ell_\pi$ rather than $L - 2\ell_\pi$, as would be suggested by a naive balancing of bulk and surface energies, was recognized first by Derjaguin [27] in 1940 and attests to the importance of long-ranged van der Waals forces in wetting phenomena. Only for exponential or finite-ranged forces is $L - 2\ell_\pi$ appropriate [27, 28].

The Kelvin equation, either the original or the modified, describes the finite-size shift of the vapour-liquid transition due to the presence of the confining walls. However, they do not tell everything about the nature of the transition. For example, reducing the slit width L leads to criticality, at which the transition disappears. For a fixed slit width L , the transition disappears

when the bulk correlation length $\xi \sim L$. A simple comparison of the two length-scales leads to finite-size scaling law which exact in the limit of $L \rightarrow \infty$:

$$T_c - T_c(L) \sim L^{-\frac{1}{\nu}}, \quad (35)$$

where ν is the correlation length critical exponent of bulk three-dimensional fluid [29, 30]. Criticality in the confined fluid lies in the two-dimensional Ising universality class. Therefore, on a critical isotherm, the adsorption should take the form

$$\Gamma \sim |\mu_c - \mu|^{1/\delta^{(2D)}} \quad (36)$$

with $\delta^{(2D)} = 15$. This gives rise to a much faster divergence of $(\partial\Gamma/\partial\mu)$ than the mean-field result which has $\delta = 3$. Moreover, the jump in adsorption should vanish as $\Delta\Gamma \sim (T_c(L) - T)^{\beta^{(2D)}}$ with $\beta^{(2D)} = 1/8$, rather than with the mean-field value $\beta = \frac{1}{2}$ or the three-dimensional value $\beta \approx 0.32$ [31].

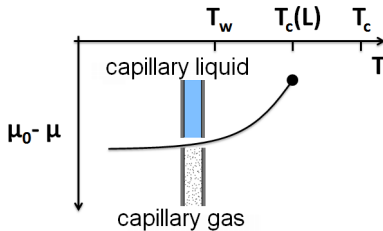


Figure 3: Schematic phase diagram of the first-order capillary condensation transition. The transition disappears at the critical temperature $T_c(L)$ which lies below the bulk critical temperature T_c and the shift is approximately given by (35). Also shown is the wetting temperature T_w which, however, does not have a considerable relevance for the transition except that for $T > T_w$ wetting layers form at the walls; in this case the modified Kelvin equation (34) is much more accurate than the original one (30).

The capillary condensation phase diagram in the plane $(T, \delta\mu)$ where $\delta\mu = \mu_0 - \mu$ is shown in Fig. 3. Not shown in this phase diagram is the prewetting first-order transition which can occur and compete with capillary condensation. However, this only occurs for very large values of the walls separations.

5 Classical Density Functional Theory

The interfacial model introduced in the previous section is a well established theoretical tool which provides us, often analytically, with a description of interfacial phenomena in terms of the interface height $\ell(\mathbf{x})$, a natural order parameter for unbinding processes such as the wetting and related transitions. For more intricate geometries and/or in cases when the inhomogeneous fluid structure due to a strong wall-fluid interaction or finite-size effects becomes important, the mesoscopic picture provided by the interfacial model may occur less satisfactory and the problem may call for more microscopic approaches based on many-body molecular Hamiltonians.

A very powerful approach to microscopic structure of inhomogeneous fluids is a density functional theory (DFT). The theory was originally developed as a quantum mechanical treatment for the ground state of inhomogeneous many-electron systems in 1960's [32, 33] and later re-formulated by Evans [34] for inhomogeneous classical fluids within a framework of statistical mechanics. Both DFT's have established as standard theoretical tools in their fields. In what follows, we will deal with the classical (statistical-mechanical) version only.

A fluid is said to be inhomogeneous if one-body density (or density distribution) $\rho(\mathbf{r})$ is spatially varying, as in the case of systems with confining walls. The one-body density is defined as

$$\rho(\mathbf{r}) = \left\langle \sum_{i=1}^N \delta(\mathbf{r} - \mathbf{r}_i) \right\rangle \quad (37)$$

where N is the number of particles and $\langle \dots \rangle$ denotes the ensemble average. Within DFT the effect of the walls is included via the external field $V(\mathbf{r})$ the walls exert. The DFT formalism establishes that for a given chemical potential μ and temperature T ($\beta = 1/k_B T$) and given inter-particle interaction $u(\mathbf{r}_i - \mathbf{r}_j)$ there is a unique intrinsic free energy functional $\mathcal{F}[\rho]$ of the density distribution $\rho(\mathbf{r})$ (and not of $V(\mathbf{r})$) and so is of the same form for any external potential. The equilibrium density distribution for the system in a given external field $V(\mathbf{r})$ is then obtained by minimizing the grand potential functional constructed from the Legendre transform of $\mathcal{F}[\rho]$:

$$\Omega[\rho] = \mathcal{F}[\rho] + \int d\mathbf{r} \rho(\mathbf{r})(V(\mathbf{r}) - \mu), \quad (38)$$

with respect to all possible functions $\rho(\mathbf{r})$. This leads to the Euler-Lagrange equation:

$$\left. \frac{\delta\Omega[\rho]}{\delta\rho(\mathbf{r})} \right|_{\rho(\mathbf{r})=\rho_{\text{eq}}(\mathbf{r})} = 0 \Leftrightarrow \mu = \frac{\delta\mathcal{F}[\rho]}{\delta\rho(\mathbf{r})} + V(\mathbf{r}) \quad (39)$$

Moreover, for the equilibrium density profile $\rho(\mathbf{r}) = \rho_{\text{eq}}(\mathbf{r})$ the grand potential functional reduces to the thermodynamic grand potential Ω .

An important feature of DFT is that it satisfies a number of the so called *sum rules*, i.e., the exact statistical mechanical relations between correlation functions and macroscopic thermodynamic quantities [35], which makes the direct link between microscopic correlations and physical properties of the macroscopic system. Particularly useful is the pressure sum rule relating the bulk pressure with the external field of the wall

$$\beta p = \int dz \rho(z) \frac{d}{dz} \exp[-\beta V(z)] \quad (40)$$

and the Gibbs adsorption theorem which connects the excess adsorption with the surface tension:

$$\Gamma \equiv \int dz (\rho(z) - \rho_b) = - \left(\frac{d\gamma}{d\mu} \right)_T, \quad (41)$$

where ρ_b is the bulk density. In both cases, a planar symmetry of the wall-fluid interface was assumed but a generalization of the theorems to other geometries is straightforward. In DFT, these sum rules are also often used as a check of numerical consistency.

Thus far, the DFT formalism has been exact and thus the exact determination of $\Omega[\rho]$ is equivalent to the full evaluation of the grand partition function:

$$Z_{\mu VT} = \sum_N \frac{e^{\beta\mu N}}{N! \Lambda^{3N}} \int \prod_{i=1}^N d\mathbf{r}_i e^{-\beta U_N}, \quad (42)$$

where

$$U_N(\mathbf{r}_1, \mathbf{r}_2, \dots, \mathbf{r}_N) = \Phi(\mathbf{r}_1, \mathbf{r}_2, \dots, \mathbf{r}_N) + \sum_i V(\mathbf{r}_i), \quad (43)$$

is the total potential of N particles including both the inter-particle interaction Φ and the external field V and Λ is the thermal de Broglie wavelength. This is, therefore, not surprising that there are no free energy functionals known

exactly except for the toy one-dimensional models. However, the strength of DFT is that on searching a suitable approximation for $\mathcal{F}[\rho]$ the well established methods from statistical physics of homogeneous fluids can be used as a guide, which makes the task much easier compared to a direct treatment of the partition function. Also note that the density distribution can be much more easily obtained from Eq. (39) than from Eq. (37).

In modern approaches, it is common to develop DFT approximations for particular classes of fluid models (rather than constructing generic approximations). Typically, the total free energy functional is split into an ideal part

$$\mathcal{F}_{\text{id}}[\rho] = \frac{1}{\beta} \int d\mathbf{r} \rho(\mathbf{r}) [\ln(\rho(\mathbf{r})\Lambda^3) - 1] \quad (44)$$

which is known exactly, and an excess part $\mathcal{F}_{\text{ex}}[\rho]$ which accounts for the interactions between the particles. For simple fluids the inter-particle potential Φ is pairwise additive and the interaction between the particles only depends on the distance between their centers. This is, e.g., the case of the well-known Lennard-Jones potential

$$u_{LJ} = 4\varepsilon \left[\left(\frac{\sigma}{r} \right)^{12} - \left(\frac{\sigma}{r} \right)^6 \right], \quad (45)$$

where the parameters ε and σ are then often used as the energy and length units.

In the spirit of van der Waals theory, the excess term of the free energy is treated in a perturbative manner, and is separated into a contribution modelling the repulsive hard-sphere (HS) core and a contribution from the attractive part $u_{\text{a}}(r)$ of the fluid-fluid intermolecular potential. This is treated most commonly in mean-field fashion:

$$\mathcal{F}_{\text{ex}}[\rho] = \mathcal{F}_{\text{HS}}[\rho] + \frac{1}{2} \iint d\mathbf{r} d\mathbf{r}' \rho(\mathbf{r}) \rho(\mathbf{r}') u_{\text{a}}(|\mathbf{r} - \mathbf{r}'|), \quad (46)$$

where $\mathcal{F}_{\text{HS}}[\rho]$ is the excess free energy functional of the hard-sphere fluid, with an appropriately chosen diameter.

Over the last three decades a number of approximative functionals for $\mathcal{F}_{\text{HS}}[\rho]$ has been proposed. Arguably the most successful one, however, is the one produced by Rosenfeld within his *Fundamental Measure Theory* (FMT)

[36]. The theory is based on an assumption that the HS free energy functional can be expressed in the form

$$\mathcal{F}_{\text{hs}}[\rho] = \frac{1}{\beta} \int d\mathbf{r} \Phi(\{n_\alpha\}). \quad (47)$$

in terms of a set of weighted densities

$$n_\alpha(\mathbf{r}) = \int d\mathbf{r}' \rho(\mathbf{r}') \omega_\alpha(\mathbf{r} - \mathbf{r}'). \quad (48)$$

Here, the six weight functions are given by

$$\omega_3(\mathbf{r}) = \Theta(R - |\mathbf{r}|), \quad (49)$$

$$\omega_2(\mathbf{r}) = \delta(R - |\mathbf{r}|), \quad \omega_2(\mathbf{r}) = \frac{\mathbf{r}}{r} \delta(R - |\mathbf{r}|), \quad (50)$$

$$\omega_1(\mathbf{r}) = \delta(R - |\mathbf{r}|), \quad \omega_1(\mathbf{r}) = \frac{\mathbf{r}}{r} \delta(R - |\mathbf{r}|), \quad (51)$$

$$\omega_0(\mathbf{r}) = \delta(R - |\mathbf{r}|), \quad (52)$$

and the function $\Phi(\{n_\alpha\})$ can be determined from dimensional analysis and from requirements that the low- and high-density limits are obeyed exactly, which leads to

$$\Phi = -n_0 \ln(1 - n_3) + \frac{n_1 n_2 - \mathbf{n}_1 \cdot \mathbf{n}_2}{1 - n_3} + \frac{n_2^3 - 3n_2 \mathbf{n}_1 \cdot \mathbf{n}_2}{24\pi(1 - n_3)^2}. \quad (53)$$

In the limit of homogeneous fluid, this result is equivalent to the compressibility Percus-Yevick equation of state [37], although modified FMT versions of even more accurate underlying equation of state are now available. Importantly, the FMT functional satisfies the sum rules, Eqs. (40) and (41) (in contrast to some alternative approximative free energy functionals).

6 Interfacial Phase Transitions: A Non-Planar Geometry

This section is devoted to interfacial phenomena that occur in systems exhibiting other than a planar symmetry. It turns out that the effect of a substrate geometry is enormous and gives rise to a number of new, geometry-driven

phenomena that, of course, are absent in the simple models described in the previous section. Although relatively new, an attempt to provide a comprehensive review of this subject would be rather challenging in view of its growing popularity in the last few years. Instead, this section illustrates my contribution to this field and thus focuses on models I have been dealing with over the last couple of years (since 2011).

6.1 Linear wedges and edges

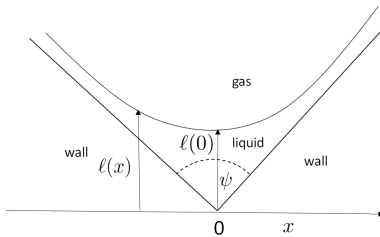


Figure 4: Schematic illustration of the meniscus height $\ell(x)$ in a linear wedge with an opening angle ψ (tilt angle $\alpha = (\pi - \psi)/2$) and $\ell_w = \ell(0)$ the equilibrium midpoint height measured above the apex.

A simple but important example of a non-planar substrate is a wedge geometry formed by two identical infinite planar walls that meet at an opening angle $\psi = \pi - 2\alpha$ where α is the tilt angle with respect to the (say) horizontal axis. The wedge geometry may be thought as being a missing link between the cases described in the previous section of a planar wall ($\alpha = 0$) and a capillary-slit ($\alpha = \pi/2$) and shows a phase transition which is distinct from both wetting and capillary condensation.

Suppose the wedge is in contact with a bulk vapour phase at temperature $T < T_c$ and chemical potential μ . Macroscopic arguments [38] dictate that at bulk coexistence, $\mu = \mu_0$, the wedge is completely filled by liquid (ℓ_w becomes macroscopically large) for all temperatures $T > T_f$ where T_f is the *filling temperature* given implicitly by the simple condition

$$\theta(T_f) = \alpha, \quad (54)$$

where $\theta(T)$ is the contact angle of a sessile drop on a flat surface. Note that (54) is consistent with and generalizes the condition for wetting transition $\theta(T_w) = 0$ and implies that $T_f < T_w$, as the contact angle decreases with temperature. Thus, the corresponding *filling transition* which occurs at T_f may be viewed as an interfacial geometry-induced unbinding transition in a system with broken translational invariance [39].

In [40, 41], the filling transitions in a right-angle wedge ($\alpha = \pi/4$) involving a long-range wall-fluid interaction were studied using a microscopic model within the density functional theory. Our DFT analysis showed that the filling transition is first order if it occurs far below the critical point but is continuous if T_f is close to T_c even though the walls still show first-order wetting behaviour. For this continuous transition the distance of the meniscus from the apex grows as

$$\ell_w \sim (T_f - T)^{-\beta_w}, \quad (55)$$

as $T \rightarrow T_f^-$, with the critical exponent estimated to be $\beta_w \approx 0.46$.

This value of the critical exponent can be compared with the mean-field value obtained from the Hamiltonian for a widely open wedge (assuming $\tan \alpha \approx \alpha$) [42, 43]

$$\mathcal{H}_w[\ell] = \int dx \int dy \left[\frac{\gamma}{2} (\nabla \ell)^2 + W(\ell - \alpha|x|) \right], \quad (56)$$

where $\ell(x, y)$ is the local height of the liquid-vapour interface relative to the horizontal. Exploiting the translation invariance of the model along the wedge, the Euler-Lagrange equation for the equilibrium profile $\ell(x)$ is:

$$\gamma \frac{d^2 \ell}{dx^2} = W'(\ell - \alpha|x|), \quad (57)$$

where the prime denotes differentiation w.r.t. ℓ . This equation, subject to the boundary conditions $\dot{\ell}(0) = 0$ and $\ell(x) \rightarrow \ell_\pi + \alpha|x|$ for $|x| \rightarrow \infty$, has the first integral:

$$\frac{\gamma \alpha^2}{2} = W(\ell_w) - W(\ell_\pi). \quad (58)$$

As $T \rightarrow T_f$, the meniscus unbinds from the wedge bottom, i.e. $\ell_w \rightarrow \infty$ and the first term on the r.h.s. becomes vanishingly small. Using Eq. (7) the result given by Eq. (54) is then immediately recovered. Furthermore, from Eq. (58)

it follows that

$$W(\ell_w) = \frac{\gamma(\alpha^2 - \theta^2)}{2} \sim \alpha - \theta(T) \text{ as } T \rightarrow T_f. \quad (59)$$

Thus, at a critical filling transition the MF value of the order parameter critical exponent is simply determined by the leading-order decay of the binding potential $W(\ell) = A/\ell^p + \dots$ by expanding the r.h.s. of Eq. (59) to first order at T_f , which yields $\beta_w = 1/p$. Recall that this result is completely different to the corresponding critical exponent for critical wetting $\beta_s = 1/(q-p)$ determined by both leading and next-to-leading order terms of the binding potential. For systems with van der Waals forces $p = 2$ and thus $\beta_w = 1/2$ ($\beta_s = 1$) which is in a good agreement with the DFT result.

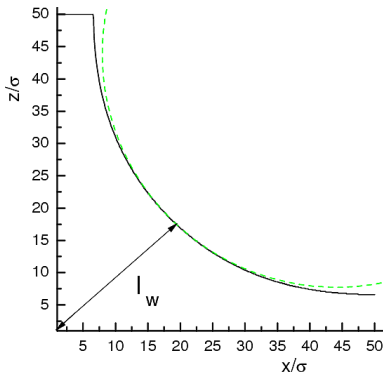


Figure 5: Contour of the meniscus as obtained from microscopic DFT. Also shown (dashed line) is a circular meniscus of Laplace radius $R = \gamma/(\delta\mu(\rho_l - \rho_g))$.

The main conclusion of this work is that it is possible to induce critical (continuous) interfacial transitions even at walls exhibiting themselves first-order wetting transitions by changing the wall geometry, which has been demonstrated for a realistic microscopic model involving dispersion interactions. It should be emphasised that for planar walls the critical wetting is a very rare

phenomenon and in fact it has not been observed on solid substrates as yet. Moreover, the influence of interfacial fluctuations for wetting transitions in three dimensions is deemed to be hardly appreciable. Therefore, the wedge structure is found to be a promising candidate for a substrate for which an observation of interfacial critical phenomena is experimentally accessible.

These findings have been extended by studying the process of complete filling, the analogy of complete wetting, i.e. the continuous divergence of the adsorption (or ℓ_w) as $\mu \rightarrow \mu_0$ for $T > T_f$. If, furthermore, $\theta = 0$, the binding potential is of the form (15) and if substituted into Eq. (58) we obtain [44]

$$\ell_w \approx \frac{\gamma(\sec \alpha - 1)}{\delta\mu(\rho_l - \rho_g)} + \frac{\sec \alpha}{1 - \beta_s^{\text{co}}} \ell_\pi + \dots \quad (60)$$

The first term in (60) is universal, i.e., it does not depend on the nature of the interactions. This leading order term can be derived using purely macroscopic concept: a meniscus that grows at the wedge corner must have a circular cross-section with radius $R = \gamma/(\delta\mu(\rho_l - \rho_f))$, as determined by the Laplace pressure difference across the interface. Figure 5 shows that this macroscopic argument is fully consistent with the microscopic DFT results and thus remains valid even on a microscopic scale. Furthermore, the height ℓ_w then follows from the condition that the meniscus must meet each side of the wedge at the correct contact angle⁹. Figure 6 reveals, however, that this macroscopically predicted value of the interface height above the wedge corner as a function of $\delta\mu$ is systematically below the DFT results.

From Eq. (60) it follows that the interfacial Hamiltonian theory extends these macroscopic results by predicting a presence of *non-universal* next-to-leading order singular term; this contribution depends on the nature of divergence of ℓ_π at a planar wall-gas interface, which in turn depends on the range of intermolecular forces (recall, $\beta_s^{\text{co}} = 1/(p + 1)$). When the non-universal correction is taken into account, one obtains a remarkably good agreement between the microscopic DFT results and Eq. (60), as shown in figure 6 for a right-angle wedge¹⁰.

⁹For general value of the contact angle, the first term would be $\frac{\gamma(\sec \alpha \cos \theta - 1)}{\delta\mu(\rho_l - \rho_g)}$.

¹⁰The results in figure 6 correspond to the model of short-range interactions, for which $\beta_s^{\text{co}} = 0$ and $\ell_\pi \sim -\ln(\delta\mu)$.

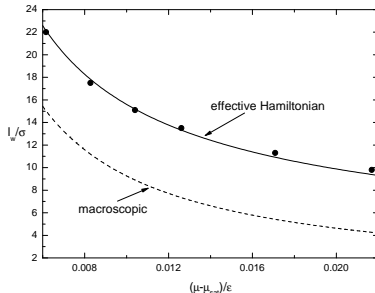


Figure 6: DFT results (symbols) for the divergence of the meniscus filling height ℓ_w , shown in comparison with the macroscopic expression given by the leading-order term in Eq. (60) (dashed curve) and the interfacial Hamiltonian prediction (solid curve) which includes the next-to-leading order correction.

Apart from the thermodynamic parameters (T, μ) , the nature of the filling transition may also be controlled by tuning the opening (tilt) angle ψ (α) of the wedge. Indeed, the relation between the temperature (via the contact angle) and the wedge opening angle is given macroscopically by (54) but this relation does not tell anything about the order of the transition. From the aforementioned studies it follows that the wedge filling transition may change its order in the proximity of T_c . However, in Ref. [45] it was shown that there exists another mechanism how to change the order of the filling transition; namely, by reducing the opening angle one can always drive the filling transition to second order implying that the adsorption continuously changes from micro- to macroscopic at T_f .

Similar conclusions have been made in Ref. [46] where we studied the effect of the external potential exerted by the walls of the wedge. We have shown that both wetting and filling transitions can be induced over a wide range of temperatures by changing the strength of the external potential. At low temperatures we find that both wetting and filling transitions are first order in keeping with predictions of simple local effective Hamiltonian models. However, close to the bulk critical point the filling transition is observed to be continuous even though the wetting transition remains first order and the wetting binding potential still exhibits a small activation barrier. The critical singularities for the mid-height of the meniscus for the continuous filling tran-

sitions depend on whether retarded or nonretarded wall-fluid forces are present and are in excellent agreement with predictions of effective Hamiltonian theory even though the change in the order of the transition is *not* anticipated (as discussed below). In particular, for retarded van der Waals forces, in which case the binding potential $W(\ell) \sim \ell^{-3}$, we have found that $\ell_w \sim (T_f - T)^{-\beta_w}$ with $\beta_w \approx 1/3$ in line with the prediction (59).

These findings are in a *partial* agreement with the predictions given by the effective Hamiltonian (56). This model also predicts a change in order from first to continuous filling, when the filling temperature T_f is sufficiently below T_w such that there is no activation barrier in the binding potential $W(\ell)$, defined for wetting at the planar wall. This is in qualitative agreement with the microscopic DFT model. However, the mechanism behind the change of order must be *different* than that within the interfacial Hamiltonian description. This is because within our microscopic study the interaction model was chosen such that the binding potential for wetting at a planar wall always has an activation barrier, thus according to the interfacial Hamiltonian model the filling transition would always be of first-order.

We believe that the reason of the discrepancy is that the original effective Hamiltonian description does not capture all the details of the filling transition. There are indeed plausible reasons for this since the original interfacial Hamiltonian model is only applicable to shallow wedges and to filling temperatures T_f far from T_c where a simple sharp-kink description of the interface structure is reliable. If the wedge is very acute or if $T_f \approx T_c$ then a sharp-kink approximation ceases to be valid. However, these are precisely the conditions where we find a change in the order of the filling transition. Extending the mesoscopic approach by adding further ingredients that are absent in (56) but that may prove to be crucial in these situations would present enormously challenging task. However, further works are needed to verify our hypothesis and a molecular simulation is perhaps the most tractable theoretical way for it.

It remains to answer a subtle question what is the precise nature of the change in order of the transition. In principle, this may happen via one of two mechanisms: a tricritical point or a critical end point. We showed that the change in the order of the filling transition occurs via a tricritical point meaning that if we were to sit along the line of first-order filling transition temperature T_f and decrease the opening angle ψ , the adsorption of the low coverage phase would diverge continuously as we approach the tricritical value

of ψ .

The effect of the opening angle was also studied in the context of surface induced freezing [48]. The value of the opening angle of the wedge was found to have a considerable effect on the structure of the confined particles in the wedge. Whether or not the crystal structure is commensurate with the wedge shape can either promote or suppress the fluid freezing. In particular, when the opening angle is around $\psi = 60^\circ$, the wedge geometry matches with the bulk crystal lattice, which strongly enhances freezing near the apex.

A specific but qualitatively different case of a linear wedge is a model with $\psi > \pi$, which we will term as an edge. As we have seen, the wedge geometry of the substrate enhances the condensation since $T_f < T_w$. In fact, the enhancement is even more effective since the filling transition is possible even in cases when the wetting transition is completely absent for any temperature $T < T_c$! This is because, the only condition to be obeyed in order the filling transition to occur is (54), no matter what the value of T_w (if any) is. The filling transition may thus be regarded as a typical example of a geometry-induced transition where both the location and order of the transition can be tuned by changing the opening angle.

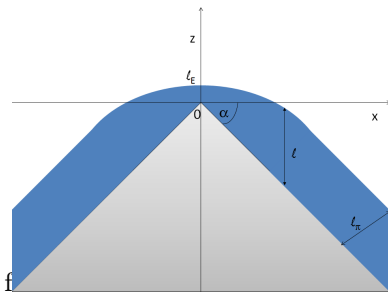


Figure 7: A sketch of the model of an edge-shaped substrate. The height of the liquid-gas interface is denoted as ℓ , the thickness of the layer far from the apex as ℓ_π and the height of the interface above the apex as ℓ_E . The sketch is projected to the x - z plane of the Cartesian coordinates.

A specific, and in some sense opposite case of the wedge model is the wall geometry characterised by the opening angle $\psi > \pi$ as represented by the sketch shown in figure 7. Now, when we consider the complete wetting scenario $\mu \rightarrow \mu_0(T)$, the curved geometry of the liquid-vapour interface dictates that the local height of the interface above the edge ℓ_E must remain finite at any subcritical temperature, even when macroscopically thick wetting films are formed far from the edge (i.e. when $T > T_w$) [47]. A natural question is: what is the height ℓ_E at a given chemical potential μ ?

This problem can be studied using the interfacial Hamiltonian model [49]

$$\mathcal{H}_e[\ell] = \int dx \left[\frac{\gamma}{2} (f'(x))^2 + W(\ell(x)) \right], \quad (61)$$

where $\ell(x)$ is the local height of the liquid-gas interface measured vertically and $f(x) = \ell(x) - \tan \alpha |x|$ denotes the local height of the liquid-gas interface relative to the horizontal plane (x axis). A translation symmetry is assumed along the edge (y -axis).

The mean-field analysis of this model shows that the equilibrium height of the interface above the edge at coexistence is given by

$$\ell_E^0 = \ell(\delta\mu = 0) = \sqrt{\frac{2a}{\gamma \tan^2 \alpha}}, \quad (62)$$

where $a(T)$ is the Hamaker constant defined by the binding potential of the corresponding planar wall $W(\ell) = A/\ell^p + \dots$. Furthermore, $\ell_E(\delta\mu)$ has been shown to approach the coexistence value according to

$$\delta\ell = \ell_E(0) - \ell_E(\delta\mu) \sim \delta\mu^{\beta_E^{\text{co}}} \quad (63)$$

as $\delta\mu \rightarrow 0^+$. The new critical exponent for complete wetting on an edge β_E^{co} depends on the range of the molecular interaction, such that $\beta_E^{\text{co}} = p/(p+1)$ and is related to the exponent α_s^{co} (defined by Eq. (12)), according to $\beta_s^{\text{co}} = 2 - \alpha_s^{\text{co}}$. For systems with van der Waals forces, $\beta_E^{\text{co}} = 2/3$. In contrast, the next-to-leading term in (63) has been found to be universal and scales linearly with $\delta\mu$, regardless of the nature of the molecular interactions.

Furthermore, using the finite-size scaling analysis, it was shown that for a substrate model that is characterised by a finite linear dimension L , the height of the interface deviates from the one at the infinite substrate as $\sim L^{-1}$ in the limit of large L . All these predictions have been fully supported by the numerical results of the microscopic density functional theory.

6.2 Capillary grooves

A further extension of the idealized planar geometries is a groove or a capped capillary formed by scoring a narrow deep channel into a solid surface. Let us now consider a macroscopically long groove of depth D and width L which is in contact with a bulk vapour and ask what is the nature of the fluid condensation inside the groove. It should be noted that the groove model, which is experimentally much more relevant than an open slit, is not only of fundamental importance but is also central to the understanding of fluids on structured surfaces which is vital for further technological applications (lab-on-a-chip technologies).

To begin, we first summarise the main properties of fluid condensation (and evaporation) in macroscopically deep grooves, $D \rightarrow \infty$, following Refs. [50, 51, 52, 53, 54, 55, 56]. It is clear that in this limit, the “boundary conditions” of the system far from the groove bottom reduce to the system of an open slit. Therefore, the groove is largely filled with capillary gas for $\mu < \mu_{cc}$ and by capillary liquid when $\mu > \mu_{cc}$. It is to be explored what is the nature of the condensation in the proximity of μ_{cc} .

First of all, two regimes – below and above the wetting temperature – have to be discussed separately.

- $T < T_w$: Below the wetting temperature, the macroscopic arguments dictate that any adsorbed liquid film has to meet the side and bottom walls in Young’s contact angle. It follows that in a low-density state two menisci form at both corners of the groove with a near-circular shape of the Laplace radius $R = \gamma/(\mu_0 - \mu)$. As the chemical potential increases towards μ_{cc} , the radius increases which means that the adsorption layers at both corners grow. However, this process must ultimately terminate when the two menisci merge, since beyond this point

$$\mu_{sp}(L) = \mu_{cc}(L) + \frac{2\gamma \sin \theta}{L\Delta\rho} \quad (64)$$

no thermodynamically stable configuration exists and the system must jump into a high-density, liquid-like state. Clearly, $\mu_{sp} > \mu_{cc}$ is the limit of the metastable extension of the low-density configuration, characteristic for *first-order* phase transitions.

- $T > T_w$. Above the wetting temperature the Young contact angle $\theta = 0$ and therefore a single meniscus at the liquid-gas interface forms near

the groove bottom. As μ tends to μ_{cc} , the process of adsorption is *continuous* and can be characterised by a growth of the meniscus height ℓ . This process thus reminds complete wetting on a planar wall, which is now shifted from μu_0 to a lower value $\mu_{cc}(L)$. However, the singular behaviour of the meniscus growth as $\mu \rightarrow \mu_{cc}$ is given by

$$\ell \sim (\mu_{cc}(L) - \mu)^{-1/4}, \quad (65)$$

and is thus characterised by a different critical exponent than complete wetting ($\beta_{co} = 1/3$).

It has also been shown that in analogy to pre-wetting the rise of the meniscus can also exhibit a finite jump. However, in contrast to pre-wetting, which is the genuine first-order transition, the transition associated with the meniscus jump must be necessarily rounded owing to its pseudo-one-dimensional nature.

Till now, we have been discussing the limit $\mu\mu_{cc}^-$ but we can also ask what happens when μ_{cc} is approached from above, i.e. the process of the liquid-like evaporation in grooves. Using the mesoscopic interfacial Hamiltonian theory, microscopic density functional theory and a dimensional analysis it has been shown that the groove evaporation is always continuous regardless of the temperature, such that the height of the meniscus from the top of the groove ℓ' decreases according to the power-law

$$\ell' \sim (\mu_{cc}(L) - \mu)^{-\beta_E}, \quad (66)$$

with a *different* critical exponent than that for groove condensation which is now $\beta_E = 1/3$ for dispersion forces, i.e., exactly the same as for complete wetting on a planar wall.

The analogy between groove evaporation and complete wetting is not accidental but in fact extends much further. It reveals that there is a precise connection between ℓ' and the film thickness on a planar wall ℓ_π :

$$\ell'(\mu - \mu_{cc}) = \ell_\pi(\mu_0 - \mu), \quad (67)$$

which is an example of a *covariance law*, revealing hidden symmetry between interfacial phenomena at different geometries.

It is also important to discuss the effect of fluctuations. The mean-field analysis neglects the long wavelength, interfacial fluctuations of the meniscus,

the most dominant of which arise from those in the height of the meniscus along the groove. Owing to a reduced effective dimensionality of the groove, the fluctuation theory of meniscus unbinding is analogous to that of two dimensional complete wetting but with a line tension, resisting the undulations of the meniscus, which is $\tau \approx \gamma L$. Therefore, the relevant effective Hamiltonian that accounts for the fluctuations in the meniscus height along the groove is now of the form

$$\mathcal{H}_g[\ell] = \int dy \left(\frac{\gamma L}{2} \left(\frac{d\ell(y)}{dy} \right)^2 + W(\ell) \right). \quad (68)$$

Using Eq. (26), the relation [26] $\xi_{\perp}^2 = k_B T \xi / \tau$ and the fact that $\xi_{\perp} \approx \ell$ when fluctuations become important, we obtain the following estimation for the fluctuation term:

$$\gamma L \ell^2 \approx \gamma L \frac{\xi_{\perp}^2}{\xi_{\parallel}^2} \approx \frac{(k_B T)^2}{\xi_{\perp}^2 \gamma L} \approx \frac{(k_B T)^2}{\ell^2 \gamma L}. \quad (69)$$

Since the binding potential for the groove evaporation reads

$$W_e \approx (\mu - \mu_{cc})(\rho_l - \rho_g)L(D - \ell) + \frac{a(T)L}{(D - \ell)^2}, \quad (70)$$

the repulsive term, which is of the order of $(D - \ell)^2$, is marginal because it is of the same order as the effective fluctuation term (69). This implies that the value of the exponent $\beta_E = 1/3$ is not altered by fluctuation effects. The only influence of the fluctuations is that the Hamaker constant becomes renormalized by a factor of $1 + \mathcal{O}((\beta \gamma L^2)^{-1})$, which is only important in the immediate vicinity of the capillary critical point.

For groove condensation, the appropriate binding potential is of the form

$$W_c \approx (\mu - \mu_{cc})(\rho_l - \rho_g)L\ell + \frac{a(T)L^2}{\ell^3} \quad (71)$$

and the repulsive term becomes irrelevant. Thus, for continuous condensation, the mean-field power-law divergence $\ell_C \approx ((\mu_{cc} - \mu)/L)^{-\frac{1}{4}}$ will eventually cross-over to $\ell_C \approx (L^2 \mu_{cc} - \mu)^{-\frac{1}{3}}$ as $\mu \rightarrow \mu_{cc}$, changing the mean-field critical exponent $\beta_C^{\text{MF}} = 1/4$ to the true value $\beta_C = 1/3$. However, a simple matching of these power laws shows that the size of the asymptotic regime is

negligibly small since it scales as L^{-11} . Thus, the mean-field description of the continuous capillary condensation is exact except for extremely close vicinity of the capillary-coexistence curve $\mu = \mu_{cc}$.

The (macroscopically deep) groove model can be extended to the case when the bottom wall interacts differently with the fluid than the side walls. This model of a heterogeneous groove [55] reveals some unexpected behaviour in the case when both types of the wall are in a complete wetting regime (i.e., the considered temperature is greater than both wetting temperatures of the walls). The relevant binding potential of the model is

$$W_{\text{cap}}(\ell) = \delta\mu(\rho_l - \rho_g)\ell + \frac{a_2 - a_1}{\ell^2} + \frac{3a_1L}{\ell^3} + \dots, \quad (72)$$

where L is the groove width and a_1 and a_2 are the Hamaker constants for the side and bottom walls, respectively. Note that the complete wetting regime requires that both a_1 and a_2 are positive. We can now identify three wetting scenarios determined by a relative strength between a_1 and a_2 :

1. For $a_1 = a_2$, i.e., in the case of a homogenous groove mentioned previously, the meniscus is repelled by a term decaying as $\sim \ell^{-3}$ which results to a continuous unbinding of the meniscus according to $\ell \sim \delta\mu^{-\frac{1}{4}}$
2. If $a_1 < a_2$, the meniscus repulsion is controlled by a term of $\mathcal{O}(\ell^{-2})$, which leads to a continuous meniscus growth according to $\ell \sim \delta\mu^{-\frac{1}{3}}$, as for complete wetting on a planar wall.
3. Finally, and most interestingly, if $a_1 > a_2$, i.e., if the fluid interaction with the side walls interaction is stronger than with the the bottom wall, the mismatch between the Hamaker constant leads to an interfacial attraction which bounds the meniscus to a finite distance even at the capillary phase boundary $\mu = \mu_{cc}^-$. Since the groove must be completely filled for $\mu = \mu_{cc}^+$, the transition is turned to be *first-order*, even though the transition would be continuous in a homogenous groove made up of either type of the wall.

The case iii) ($a_1 > a_2$) has remarkable repercussions: as the fluid state remains in the partial wetting state, it is possible – in analogy with Young’s equation (3) – to define a *capillary contact angle*:

$$\gamma_{\text{wg}}(L) = \gamma_{\text{wl}}(L) + \gamma(L) \cos \theta^{\text{cap}}, \quad (73)$$

valid for $\mu = \mu_{cc}$. Here, the capillary surface tensions $\gamma_{wg}(L)$, $\gamma_{wl}(L)$ and $\gamma(L)$ are the surface free energies between groove bottom and capillary gas, groove bottom and capillary liquid and capillary gas and capillary liquid, respectively, per unit area of the groove bottom. For sufficiently wide grooves, the meniscus cross-section is near circular and thus $\gamma(L) \approx \pi/2\gamma$.

Therefore, somewhat counter-intuitively, if the attraction of the bottom wall is weaker than the attractive strength of the side walls, a liquid-vapour interface of a non-zero capillary contact angle forms in the groove even though $\theta^{\text{cap}} = 0$ for the grooves of either material.

Let us now turn to the case of finite D , which effectively means that we are considering microscopically deep grooves. It was shown [56] that the partial wetting regime ($T < T_w$) the condensation occurs at the pressure given by *modified Kelvin equation*

$$p_{cc}(L, D) = \frac{2\gamma \cos \theta_E}{L} \quad (74)$$

which has the same form as the standard Kelvin equation but is expressed in terms of the *edge contact angle* θ_E , rather than Young's contact angle θ , and the concept of which has been originally proposed in Ref. [57] for the model of open slits of finite heights. The relation between θ and θ_E is only via the aspect ration L/D . In the condensed state, the meniscus is pinned at the edges of the groove (the free energy acquires a minimum in this state) except for Young's contact angle $\theta = \theta^* \approx 31^\circ$ in which case the local pinning (and the free energy barrier) vanishes. For this value of the contact angle the meniscus can be arbitrarily moved upwards or downwards without any free-energy cost and thus represents a Goldstone mode for condensation transition in capillary grooves. Moreover, the nature of the condensation turns out to be qualitatively different below and above θ^* . In both cases, the asymptotic value of the condensation pressure in the limit of $D \rightarrow \infty$ is the standard Kelvin pressure (given by the classical Kelvin equation) but is approached from below if $\theta < \theta^*$ and from above if $\theta > \theta^*$.

It should be emphasised that the value of the threshold Young's contact angle $\theta^* \approx 31^\circ$ is *universal*, i.e. identical for any fluid and any wall material; it only depends on the groove geometry. Our arguments have been supported by detailed microscopic density functional theory calculations which show that the modified Kelvin equation remains highly accurate even when L and D are of the order of tens of molecular diameters.

6.3 Rough surfaces

We now extend the model of a single groove to a periodic system formed by a one-dimensional array of parallel (infinitely long) grooves. The complete wetting process, $\mu \rightarrow \mu_0^-$ with $T > T_w$ becomes considerably richer now and can be summarised as follows [58, 59, 60]:

1. It is possible to distinguish between four different wetting regimes:
 - (a) *Empty grooves*: In this low-density state ($\mu \ll \mu_0$) the grooves are filled essentially by the capillary gas with only a microscopic adsorption of the liquid phase near the groove corners.
 - (b) *Filled grooves*: In this state, the grooves are filled with capillary liquid but the top of the walls is only partially wet, i.e. covered by only a microscopic amount of liquid.
 - (c) *Edge pinning*: As the chemical potential is increased still more, the top of the grooves becomes wet, since the binding potential for the corresponding planar wall is repulsive. However, the presence of the groove edges prohibits complete wetting and the liquid-gas interface is pinned at the edges giving rise to a periodic array of cylindrical droplets.
 - (d) *Complete wetting*: Sufficiently close to μ_0 , the liquid-gas interface unbinds from the groove edges as followed by a further growth of the wetting film similarly to complete wetting on a flat wall. However, the interface remains undulated and flattens continuously.
2. On a mesoscopic level, the wetting temperature, at which the wall is completely wet in the limit of $\mu \rightarrow \mu_0$, is the same as for the planar wall. However, the microscopic analyses have shown that the structure of the wall may substantially decrease the wetting temperature [59, 60].
3. There is a *qualitative* discrepancy between the microscopic results of adsorption on microscopically structured (rough) walls and the macroscopic predictions. In particular, a contact angle θ_E of a sessile drop within a purely phenomenological (thermodynamic) treatment is given by the Wenzel law [61], according to which

$$\cos \theta_E = r \cos \theta \tag{75}$$

where θ is Young's contact angle of the pertinent flat wall and $r \geq 1$ is a parameter which characterises the wall roughness ($r = 1$ for a flat wall). According to this law, the structure of the wall enhances the "hydrophilic" character of the wall, i.e. $\theta_E < \theta$ for $\theta < \pi/2$. However, for microscopically corrugated walls, the microscopic analyses showed the opposite, i.e. that the contact angle increases with the wall roughness, and indeed so much so, that the wall may become "hydrophobic" ($\theta_E > \pi/2$) for r large enough [59].

6.4 Bridging transitions

As a final example of the interfacial phase transitions we discuss the process during which two wetting films merge to form a single one. From a purely macroscopic viewpoint this so called *bridging transition* is always of first-order in view of the change of the wetting geometry. However, a more detailed analysis shows that the transition may be first-order, rounded or critical depending on the geometric properties of the wetted bodies.

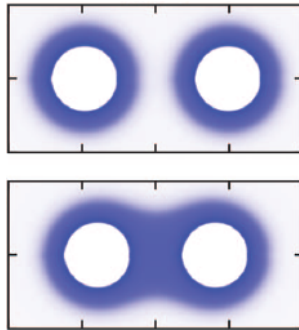


Figure 8: A sketch representing unbridged (top) and bridged (bottom) states of two spherical colloids immersed in a solvent.

Consider first two large spherical bodies (colloids, nanoparticles...), each of a radius R , embedded into a sea of small particles (solvent) at two-phase

bulk coexistence $\mu = \mu_0$. If the separation between the colloids H is large enough, two separate spherical wetting layers form around each of the colloids of the width depending on R and the microscopic forces. In particular, in the presence of long-range dispersion-like (solvent-solvent or colloid-solvent) forces, the width of the wetting layers grow as $R^{1/3}$ for large R [62, 63]. In contrast, if only short-range forces (i.e. of finite range or decaying exponentially at large distances) are present, the wetting layers grow logarithmically with R . However, as the colloids get closer together, their wetting layers merge and the bridging transition occurs at a certain distance H_b .

As was shown in Ref. [64], there exists a critical radius R_c of the colloids, such that for $R > R_c$ the transition is first-order and reminds capillary condensation (clearly, the two transitions become identical in the limit of $R \rightarrow \infty$). However, for $R < R_c$ the transition is continuous (rounded). The nature and the location of the transition have been subsequently worked out in Ref. [65]. It was shown that for the spherical colloids the shape of the bridging film is a catenoid formed by rotating the catenary $y = a \cosh \frac{x}{a}$ about the revolution x axis connecting the centers of the spheres. The distance H_b at which the bridging transition occurs was shown to scale linearly with R according to

$$H_b/R = \alpha(\theta) \quad (76)$$

where the function α only depends on temperature via the Young contact angle θ . In particular, if the spherical colloids are completely wet ($\theta = 0$), $\alpha \approx 2.32$, while for neutral wetting, $\theta = \pi/2$, $\alpha = 2$ meaning that no bridging occurs.

Similar results apply for a pair of parallel cylindrical colloids. In this case, the bridging transition occurs at an axis-to-axis distance

$$H_b/R = (\pi - 2\theta) \cos \theta + 2 \sin \theta \quad (77)$$

where R is the radius of the cylinders. Note that $H_b = 2R$, again, for neutral wetting ($\theta = \pi/2$) while $H_b = \pi R$ for complete wetting ($\theta = 0$).

These results can be further corrected by considering influence of the singular part of the surface free energy arising from complete wetting layers. This contribution shifts the phase boundary by multiplying the r.h.s. of (76) and (77) by factor $\xi_l/(2R) \ln(R/\xi_l)$ and $\xi_l/R \ln(R/\xi_l)$, respectively, where ξ_l is the liquid correlation length of the solvent. Note that the different prefactor of the corrections reflects the difference in the curvature between the spheres and cylinders.

Although the location of the bridging transitions is similar for cylinders and spheres, all other aspects, particularly the stability of liquid bridges, are very different in the two systems. In both cases, the bridged configuration can extend into metastable region for $H > H_b$. The mechanism of these extensions are different, though. For spheres, there always exists a limit-of-stability H_s where the catenoid ceases to have solution touching the spheres and for complete wetting regime $H_s \approx 2.38R$; the metastable region is thus very narrow. In contrast, the shape of the bridging film between two cylinders is flat which has always a solution and thus the metastable region $H > H_b$ is unbounded. Only off the bulk two-phase coexistence, in which case the liquid-gas interface forming the liquid bridging film is not flat but rather an arc of the Laplace radius, there exists the end-of-the-stability which corresponds to pinching of the bridge film where the two arc circles meet.

7 Conclusion

The presented dissertation summarizes the main of the author contribution to the theory of interfacial phenomena at geometrically structured surfaces and the selected articles all belong to this research area. They illustrate complexity of these phenomena are a dramatic impact of the wall geometry; the chosen model substrates are shown to induce some new types of phase transitions and criticality that have no analogy in bulk or at planar surfaces. However, although the studied phenomena appear to be very specific for the given substrate geometry, there exists “covariance laws” revealing striking symmetries and deep connections between fluid phase behaviour in very distinct systems. There is obviously many more physically relevant models that are still largely unexplored, especially from a microscopic perspective which would link the phenomenology of the observed fluid behaviour with the microscopic forces acting between fluid and wall molecules. This understanding is of a fundamental theoretical interest but there are also promising perspectives in applications for modern technological branches dealing with fabrication of “smart surfaces” that is of the central interest in the modern material science. All these challenges bring about ever increasing popularity of the field among physicists, chemists and engineers. Dynamical behaviour of the corresponding non-equilibrium systems is another area of rapidly growing interest which, however, goes beyond the scope of the dissertation.

8 List of selected publications

1. Malijevský Alexandr and Parry Andrew: Critical Point Wedge Filling, *Phys. Rev. Lett.* **110**, 166101 (2013).
2. Malijevský Alexandr and Parry Andrew: Density functional study of complete, first-order and critical wedge filling transitions, *J. Phys.: Condens. Matter* **25**, 305005 (2013).
3. Malijevský Alexandr and Parry Andrew: Filling transitions in acute and open wedges, *Phys. Rev. E* **91**, 052401 (2015).
4. Malijevský Alexandr and Parry Andrew: Influence of intermolecular forces at critical-point wedge filling, *Phys. Rev. E* **93**, 040801(R) (2016).
5. Archer Andrew and Malijevský Alexandr: Crystallization of soft matter under confinement at interfaces and in wedges, *J. Phys.: Condens. Matter* **28**, 244017 (2016).
6. Malijevský Alexandr: Complete wetting near an edge of a rectangular-shaped substrate: *J. Phys.: Condens. Matter* **26**, 315002 (2014).
7. Malijevský Alexandr: Does adsorption in a single nanogroove exhibit hysteresis?, *J. Chem. Phys.* **137**, 214704 (2012).
8. Malijevský Alexandr and Parry Andrew: Condensation and evaporation transitions in deep capillary grooves, *J. Phys.: Condens. Matter* **26**, 355003 (2014).
9. Parry Andrew, Malijevský Alexandr and Rascón Carlos: Capillary Contact Angle in a Completely Wet Groove, *Phys. Rev. Lett.* **113**, 146101 (2014).
10. Malijevský Alexandr, Parry Andrew, and Pospíšil Martin: Edge contact angle and modified Kelvin equation for condensation in open pores, *Phys. Rev. E* **96**, 020801(R) (2017).
11. Malijevský Alexandr and Parry Andrew: Modified Kelvin Equations for Capillary Condensation in Narrow and Wide Grooves, *Phys. Rev. Lett.* **120**, 135701 (2018).

12. Malijevský Alexandr: Filling and wetting transitions at grooved substrates, *J. Phys.: Condens. Matter* **25**, 445006 (2013).
13. Malijevský Alexandr: Does surface roughness amplify wetting?, *J. Chem. Phys.* **141**, 184703 (2014).
14. Svoboda Martin, Malijevský Alexandr and Lísal Martin: Wetting properties of molecularly rough surfaces, *J. Chem. Phys.* **143**, 104701 (2015).
15. Nold Andreas, Malijevský Alexandr, and Kalliadasis Serafim: Wetting on a spherical wall: Influence of liquid-gas interfacial properties, *Phys. Rev. E* **84**, 021603 (2011).
16. Malijevský Alexandr: Effective interactions between a pair of colloids, *Mol. Phys.* **113**, 1170 (2015).
17. Malijevský Alexandr and Parry Andrew: Bridging transitions for spheres and cylinders, *Phys. Rev. E* **92**, 022407 (2015).

References

- [1] J. W. Cahn, J. Chem. Phys. **66**, 3667 (1977).
- [2] G. F. Teletzke, L. E. Scriven, and H. T. Davis, J. Coll. Int. Sci. **87**, 550 (1982).
- [3] D. E. Sullivan, Phys. Rev. B **20**, 3991 (1979).
- [4] D. E. Sullivan, Faraday Symp. **216**, 191 (1981).
- [5] D. E. Sullivan, J. Chem. Phys. **74**, 2604 (1981).
- [6] H. Nakanishi and M. E. Fisher, Phys. Rev. Lett. **49**, 1565 (1982).
- [7] P. Tarazona and R. Evans, Mol. Phys. **48**, 799 (1983).
- [8] D. Bonn, J. Eggers, J. Indekeu, J. Meunier, and E. Rolley, Rev. Mod. Phys. **81**, 739 (2009).
- [9] T. Yanagishita, K. Nishio, and H. Masuda, Adv. Mater. **17**, 2241 (2005).
- [10] A. S. Urban, A. A. Lutich, F. D. Stefani, and J. Feldmann, Nano Lett. **10**, 4794 (2010).
- [11] H. Bruus, *Theoretical Microfluidics*, Oxford University Press, (2007).
- [12] C. Rascón, A. O. Parry, and A. Sartori, Phys. Rev. E **59**, 5697 (1999).
- [13] T. Andrews, Philosophical Transactions of the Royal Society of London **159**, 575 (1869).
- [14] J. D. van der Waals, *Over de Continuïteit van den Gas- en Vloeïstofoestand*, PhD thesis, Leiden, The Netherlands (1873).
- [15] L. D. Landau, Zh. Eksp. Teor. Fiz. **7**, 19 (1937).
- [16] J. R. Baxter, *Exactly solved models in statistical mechanics* London: Academic Press Inc. (1982).
- [17] L. Onsager, Physical Review **65**, 117 (1944).
- [18] B. Widom, J. Chem. Phys. **43**, 3892 (1965).

- [19] L. P. Kadanoff, *Physics* **2**, 263 (1966).
- [20] K. G. Wilson, *Physical Review B*. **4**, 3174 (1971).
- [21] K. G. Wilson, *Physical Review B*. **4**, 3184 (1971).
- [22] K. G. Wilson and M. E. Fisher, *Phys. Rev. Lett.* **28**, 240 (1972).
- [23] D. E. Sullivan and M. M. Telo da Gama, in *Fluid Interfacial Phenomena*, edited by C. A. Croxton (Wiley, New York, 1985)
- [24] S. Dietrich, in *Phase Transitions and Critical Phenomena*, edited by C. Domb and J. L. Lebowitz (Academic, New York, 1988), Vol. 12.
- [25] M. Schick, in *Liquids and Interfaces*, edited by J. Chorvolin, J. F. Joanny, and J. Zinn-Justin (Elsevier, New York, 1990).
- [26] R. Lipowsky and M. E. Fisher, *Phys. Rev. B* **36**, 2126 (1987).
- [27] B. V. Derjaguin, *Acta Phys. Chem.* **12**, 181 (1940).
- [28] R. Evans and U. Marini Bettolo Marconi, *Chem. Phys. Lett.* **114**, 415 (1985).
- [29] M. E. Fisher and H. Nakanishi, *J. Chem. Phys.* **75**, 5857 (1981).
- [30] H. Nakanishi and M. E. Fisher, *J. Chem. Phys.* **78**, 3279 (1983).
- [31] R. Evans, *J. Phys.: Condens. Matter* **2**, 8989 (1990).
- [32] P. Hohenberg and W. Kohn, *Physical Review*. **136**, B864 (1960).
- [33] W. Kohn and L. J. Sham, *Physical Review*. **140**, A1133 (1965).
- [34] R. Evans, *Adv. Phys.* **28**, 143 (1979).
- [35] D. Henderson, *Fundamentals of Inhomogeneous Fluids*, Marcel Dekker, New York (1992).
- [36] Y. Rosnefeld, *Phys. Rev. Lett.* **63**, 980 (1989).
- [37] J.-P. Hansen and I. R. McDonald, *Theory of simple fluids*, Academic Press, Oxford (2013).

- [38] E. H. Hauge, Phys. Rev. A **46**, 4994 (1992).
- [39] K. Rejmer, S. Dietrich, and M. Napiorkowski, Phys. Rev. E **60**, 4027 (1999).
- [40] A. Malijevský and A. O. Parry, Phys. Rev. Lett. **110**, 166101 (2013).
- [41] A. Malijevský and A. O. Parry, J. Phys.: Condens. Matter **25**, 305005 (2013).
- [42] A. O. Parry, C. Rascón, and A. J. Wood, Phys. Rev. Lett. **83**, 5535 (1999).
- [43] A. O. Parry, C. Rascón, and A. J. Wood, Phys. Rev. Lett. **85**, 345 (2000).
- [44] C. Rascón and A. O. Parry, Phys. Rev. Lett. **94**, 096103 (2005).
- [45] A. Malijevský and A. O. Parry, Phys. Rev. E **91**, 052401 (2015).
- [46] A. Malijevský and A. O. Parry, Phys. Rev. E **93**, 040801(R) (2016).
- [47] A. O. Parry, M. J. Greenall, and J. M. Romero, Phys. Rev. Lett. **90**, 046101 (2003).
- [48] A. Archer and A. Malijevský Alexandr, J. Phys.: Condens. Matter **28**, 244017 (2016).
- [49] Malijevský Alexandr, J. Phys.: Condens. Matter **26**, 315002 (2014).
- [50] M. Tasinkevych and S. Dietrich, Eur. Phys. J. E **23**, 117 (2007).
- [51] A. O. Parry, C. Rascón, N. B. Wilding, and R. Evans, Phys. Rev. Lett. **98**, 226101 (2007).
- [52] A. Malijevský, J. Chem. Phys. **137**, 214704 (2012).
- [53] A. Malijevský, J. Phys.: Condens. Matter **25**, 445006 (2013).
- [54] A. Malijevský and A. O. Parry, J. Phys.: Condens. Matter **26**, 355003 (2014).
- [55] A. O. Parry, A. Malijevský, and C. Rascón, Phys. Rev. Lett. **113**, 146101 (2014).

- [56] A. Malijevský and A. O. Parry, *Phys. Rev. Lett.* **120**, 135701 (2018).
- [57] A. Malijevský, A. O. Parry, and M. Pospíšil Martin, *Phys. Rev. E* **96**, 020801(R) (2017).
- [58] A. Malijevský, *J. Phys.: Condens. Matter* **25**, 445006 (2013).
- [59] A. Malijevský, *J. Chem. Phys.* **141**, 184703 (2014).
- [60] M. Svoboda, A. Malijevský, and M Lísal Martin, *J. Chem. Phys.* **143**, 104701 (2015).
- [61] R. N. Wenzel, *Ind. Eng. Chem.* **28**, 988 (1936).
- [62] M. C. Stewart and R. Evans, *Phys. Rev. E* **71**, 011602 (2005).
- [63] A. Nold, A. Malijevský, and S. Kalliadasis Serafim, *Phys. Rev. E* **84**, 021603 (2011).
- [64] A. Malijevský Alexandr, *Mol. Phys.* **113**, 1170 (2015).
- [65] A. Malijevský and A. O. Parry Andrew, *Phys. Rev. E* **92**, 022407 (2015).